Evaluating the use of NMR for the determination of deuterium abundance in water

University of Groningen

university of groningen

faculty of science and engineering

Alex Martínez

11 July 2022

Abstract

Nuclear Magnetic Resonance (NMR) is in use by a few laboratories in Europe to quantitatively measure the site-specific isotopic composition of samples containing one or more NMR-active nuclei. The aim of this project was to explore whether this could be applicable to water isotope research at the University of Groningen. The study of isotopes, and particularly water, has a variety of applications, ranging from food authentication and medicine to climate science. The use of NMR in this field instead of more conventional alternatives like mass spectrometry would offer several advantages, such as site-specific information and non-destructive measurements. In addition, successful NMR isotope measurements on water would be the st-up to more complicated molecules such as ethanol.

Thus, quantitative deuterium isotopic abundance experiments were performed using a Bruker 600MHz NMR instrument and the data analysed using the MestReNova software. Initially no reference compound was used, and later acetonitrile was added as an internal reference with a customised isotopic abundance. Measurements were performed with a set of water samples and then calibrated. Results showed a wide spread in the peak area between different measurements, which was affected by integration limits and waiting time before the first experiment, among other factors. Deuterium peak areas were more variable for higher integral limits, while for proton the change in precision was not as significant. Final results showed a desirable accuracy in three out of four water samples, but standard deviation of each sample remained higher than would be desirable. Further research should thus focus on increasing the stability of this technique.

Acknowledgements

First of all, I would like to thank my supervisors, Prof. Dr. H. A. J. Meijer and Dr. D. Paul. Prof. Dr. H. A. J. Meijer welcomed me into the Centre for Isotope Research and offered great feedback and support during all the project. Dr. D. Paul helped me through the daily experiments and results and taught me how to work in the laboratory, and his guidance proved invaluable for this research project. Second, I would like to thank Dr. J. Kemmink and Ing. P. van der Meulen, who taught me how the NMR functions and solved all our questions and problems with it. I would also like to mention Ing. A.C. van Buuren, who helped with the measurements with the Liquid Water Isotope Analyzer. Finally, I would like to thank the Center for Isotope Research and Groningen University for giving me the opportunity to complete this project.

Contents

Chapter 1

Introduction

The aim of this project was to study and understand how NMR could be used in a quantitative way to measure stable isotope abundances, in particular, singly-substituted deuterium containing isotopologues of water. Additionally, the goal was to investigate whether this technique, available at the Stratingh Institute for Chemistry, is accurate and precise enough to be useful to the research performed at the Centre for Isotope Research in Groningen.

On the one hand, NMR is a technique which measures the oscillation of the magnetisation of the sample under a magnetic field [1]. First, the sample is placed under a strong magnetic field, which aligns the spins of its nuclei with the field, inducing a net magnetisation in the same direction. Then, the application of a perpendicular RF pulse tilts the magnetisation vector, resulting in oscillations. The key advantage is that this second perpendicular field does not need to be as strong as the main one to create a significant tilt. Since the frequency of the oscillations depends on the spin and coupling of a particle with its neighbours, every molecule and position upon it will result in a different peak in the measured spectrum.

There are several advantages associated with the use of NMR instead of other more conventional techniques [2]. Firstly, since it is non-invasive, the sample is not destroyed during the experiment and can be repeatedly measured and retrieved after use. This is especially useful when the sample availability is limited. In contrast, mass spectrometry, which is often used to verify results, is a destructive technique. Secondly, NMR imaging provides site specific information, as each position in the molecule generates a distinct peak in the spectra. This can later be used, for instance, to determine the purity of the sample. On top of this, NMR can measure several

different substances in the sample at the same time, offering a wide range of information.

On the other hand, isotopic fractionation allows a high degree of traceability in stable isotope research. Different isotopes of an element, having different masses and binding energies, behave differently under the same physical and chemical processes [3]. Similar samples of a substance from different origins naturally contain varying abundances of certain isotopes, thus the origin and history of a sample can be determined by its specific isotope abundances. These isotope abundances are expressed through the isotopic ratio, the ratio between the concentrations of rare and abundant isotope. In order to facilitate comparison and standardisation, the delta value is used to express the isotopic ratio with respect to an international reference, as will be explained in later sections.

Due to the aforementioned traceability, isotope research has proven to be of great utility across many different fields of study. In particular, stable water isotope research has a wide range of applications, from biology [4] to oenology [5], where it is used to authenticate the origin of wine products. For instance, it is commonly used in climate science, since natural abundances of stable isotopes suffer small variations caused by the specific physical and biogeochemical processes they undergo. Examples of its use include the determination of the origin and evolution of pollutants [6] or reconstruction of the water cycle [7].

The use of Nuclear Magnetic Resonance for the study of natural isotope fractionation was first proposed by Martin et al. in 1981 [8], where deuterium spectra of ethyl derivatives where studied. Since then, the field has grown and become a standard method used in various areas, and in particular, food origin authentication [9]. In recent years, advances in measurement precision and processing software have led to the spread of quantitative NMR (q-NMR), which uses the obtained spectra to measure quantitatively the concentration of chemical species in the solution [10].

As a result, it is clear that NMR could offer a number of benefits to the Centre for Isotope Research. This technique is routinely used by several institutes within the University of Groningen, like the Stratingh Institute for Chemistry, but has yet not been used for quantitative measurements of isotope abundance. This would require a precision of the delta values under five permille points. Therefore, it is the goal of this project to study whether it would be possible to apply NMR experiments for quantitative isotope research, starting with singly-substituted deuterium isotopologues of water.

Chapter 2

Theory

2.1 Nuclear Magnetic Resonance

Nuclear Magnetic Resonance (NMR) is a technique which measures the oscillation of the magnetization of a sample under a magnetic field. Most of this section is based on the book *Understanding NMR spectroscopy* by J. Keeler [1].

Every nucleus has a certain intrinsic nuclear spin, determined by the spins of its proton and neutrons, as shown in Table 2.1. This nuclear spin results in a nuclear magnetic moment. Under a magnetic field, it is energetically favourable for these moments to align with the external field. Macroscopically, the material acquires a certain magnetization, which is proportional to the magnetic field vector. The proportionality constant is given by its susceptibility, which depends on the properties of the material.

If the magnetization has a different orientation to the magnetic field, the magnetic field will exert a torque over the magnetization which will cause it to precess around its axis. This is called Larmor precession, and the frequency of the oscillations is the Larmor frequency. The proportionality between magnetic field and precession frequency is given by the gyromagnetic ratio, which depends on spin, charge and mass, among others. Therefore, the frequency is characteristic for every nucleus. Furthermore, some isotopes, having no nuclear spin, are NMR inactive, like ^{12}C and ^{16}O, as shown in Table 2.1. In contrast, isotopes such as proton and deuterium have different nuclear spins, so they oscillate at different frequencies.

In a NMR spectrum, these frequencies are measured for every element,

Isotope	Nuclear spin
^{1}H	1/2
^{2}H	1
^{12}C	0
^{13}C	1/2
^{14}N	1
^{15}N	1/2
^{16}O	0
^{17}O	3/2

Table 2.1: Examples of nuclear spins of some isotopes [11]. Nuclear spin depends on the spins of protons and neutrons, and is therefore a integer multiple of 1/2.

both qualitatively and quantitatively. If a nucleus has gyromagnetic ratio γ, the frequency ν under a magnetic field B will be given by:

$$\nu = -\frac{1}{2\pi} \cdot \gamma \cdot B \tag{2.1}$$

Since the oscillating frequencies are proportional to the magnetic field and vice versa, the magnetic field is usually expressed in frequency units. In addition, instead of working with absolute frequencies, as the differences are relatively small, it is common practice to express them relative to a reference value, the chemical shift, which is expressed in ppm:

$$\delta = \frac{\nu - \nu_{ref}}{\nu_{ref}} \tag{2.2}$$

When the experiment starts, a strong and homogeneous magnetic field B_0 is applied, which induces the magnetization M of the sample in the same direction, as represented in Figure 2.1. However, for the oscillations to start, this vector has to be tilted with respect to the external field. To do so, a second, perpendicular magnetic field B_1 is applied, which oscillates near the Larmor frequency of the sample. The key element of the NMR technique relies on the fact that, classically, in the frame rotating with the frequency of the second field B_1, the main magnetic field B_0 appears to shrink. This allows to tilt the magnetization applying precisely timed perpendicular RF pulses, which can be weaker than the main field as long as the frequency is close to the Larmor frequency.

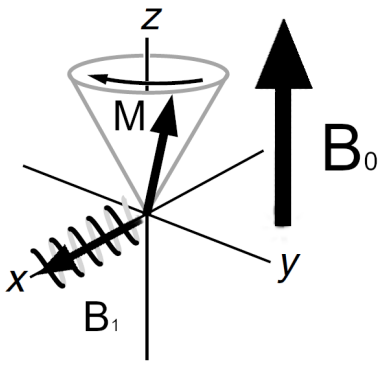

Figure 2.1: Schematic drawing of the magnetic field and magnetization in an NMR experiment. B_0 is the main magnetic field applied by the NMR. A coil surrounds the sample and is used to induce a second, oscillating magnetic field B_1. This causes the tilt of the magnetization M. As the magnetization precesses, it induces a current on the coil, which is then detected. Image adapted from [1]

This can be explained by two different interpretations. On the one hand, the situation can be roughly explained from a classical point of view. The oscillating field B_1 can be viewed as a sum of two fields rotating in opposite directions in the plane perpendicular to the magnetization. This allows us to analyse the situation in a reference frame that rotates at the same frequency as one of the rotating fields, eliminating the time dependence. In this frame, as in any rotating frame, the Larmor frequency is modified. In fact, if the rotations had the same frequency as the Larmor frequency, the apparent Larmor frequency would be zero. Therefore, since the Larmor frequency is directly proportional to the main magnetic field B_0, this field also appears to shrink in the rotating frame. The closer the oscillations of the second field are to the Larmor frequency, the smaller the apparent Larmor frequency in the rotating frame is and the smaller the apparent reduced field experienced is. As a result, the effective field, which is the sum of both field B_0 and B_1, is no longer in the direction of the magnetization, but it is lying close to its perpendicular plane, and, thus, produces a torque over it, tilting it.

The pulse length determines the tilt angle of the magnetization. This allows for different combinations of pulses, such as a ninety-degree pulse, which gives the maximum intensity. Once the pulse sequence is over, the oscillating magnetic field is turned off. Then, the system returns to the initial

setup but with the key difference that the magnetization vector is tilted by a certain angle with respect to the magnetic field, so it will start to precess around it. As it precesses, the tilt angle of the magnetization will gradually decrease through a process called relaxation. Thus, the amplitude of the signal will gradually decrease with time. The time it takes for a nucleus to return to its original state is the relaxation time. Usually, the sample is left to rest for around five times the relaxation time between each measurement to ensure that all the sample has been deexcited.

On the other hand, a complete explanation requires a quantum mechanical interpretation. As an example, we will analyse a nucleus with two possible spin values. When a magnetic field is applied, the energy level is split in two, corresponding to parallel or antiparallel spin. When the second, oscillating, weak magnetic field B_1 is applied, it introduces a perturbation, so these two levels are no longer eigenstates. If the second field oscillates at the same frequency as the Larmor frequency, the system is in resonance and the probability of transitioning from the parallel to antiparallel state is maximal. This transition emits a photon with an energy corresponding to the difference between the two levels, which is proportional to the Larmor frequency, leading to the detected signal.

For systems with multiple spins, the energy level splitting becomes more complex, resulting in a spectrum with more peaks and information. For example, a two-spin system would result in a doublet of doublets. Each doublet would be centred in its corresponding chemical shift and split in two by the scalar coupling between the spins. For more complex systems, the spectrum is determined by the scalar coupling and shielding between the neighbouring nuclei.

As a consequence of the coupling and shielding, each nucleus experiences a different effective magnetic field, resulting in different Larmor frequencies and chemical shifts. Therefore, one of the advantages of NMR is that it can give site specific information about the molecule, since each position will have a different environment and splitting.

In an NMR spectrum, the area of a peak is directly proportional to the number of particles excited. Quantitative NMR takes advantage of this to measure concentration of compounds in a sample.

The experimental setup of the NMR spectrometer has several components. First of all, a superconducting magnet is needed to produce the main, strong magnetic field. This has to be as homogeneous as possible, otherwise the spectral line shape would be distorted, leading to a poor resolution and

sensitivity. Therefore, shimming is applied to correct any inhomogeneities. This is performed through a series of coils that surround the magnet and that are adjusted to introduce the necessary corrections.

Secondly, as we have mentioned, a perpendicular field has to be applied. This is done by surrounding the sample with a coil, which can be used to both create the RF field and then detect the signal induced by the oscillating magnetization. In addition to this, the setup also includes a variety of other components to amplify and control the signal, and transmit it into a computer. The signal is recorded in the time domain, and is later Fourier transformed into a frequency spectrum by the processing programme.

Another important aspect to obtain high resolution spectra is correcting the drift of the magnet. Due to instabilities, the magnetic field drifts over the measurements, which causes the peaks in the spectrum to be broadened, reducing the resolution. To keep the measurements more stable, signals are measured with respect to a reference signal (the lock signal, usually the signal of the solvent). This enables the correction of the magnetic field to keep the lock signal in the same position, correcting the drift.

2.2 Isotopic Fractionation

Physical and chemical properties of atoms are mostly determined by their number of protons and electrons. However, isotopic mass also causes measurable differences in their response to these processes. In general, the most stable configuration for light elements tends to have the same number of protons and neutrons (^1H,^{12}C,$^{14}N^{16}O$). In some cases, having a different number of neutrons can also be stable (^2H,^{13}C,^{18}O), although their natural concentration is smaller as during nucleosynthesis their production was less favourable. In other cases, isotopes can be unstable and decay by radioactive processes (^3H,^{14}C), which results in many orders of magnitude lower natural concentrations. In both cases, the small differences between isotope species result in variations of their natural abundance, via a process known as isotope fractionation. This section is based on the book *Principles of Isotope Hydrology* by Prof. Dr. W. G. Mook [3].

As mentioned, isotope fractionation is caused by differences between isotopes. Molecules containing heavier isotopes have a higher mass, which results in a lower mobility. Consequently, they have lower diffusion velocity and their collision frequency, which determines their reaction rate, is smaller.

Furthermore, heavier molecules generally have a higher binding energy, further decreasing the reaction rate. In some special cases, the light isotope is more tightly bound, resulting in inverse isotopic fractionation.

Fractionation is temperature dependent, and usually decreases with increasing temperatures. This is because the binding energy becomes smaller compared to thermal energy, which is mass independent, and so, the mass difference becomes less important.

The effects of isotopic fractionation are usually described quantitatively by the isotopic fractionation factor:

$$\alpha = \frac{R_A}{R_B} \tag{2.3}$$

Where R_i are the isotopic ratios of the compounds, defined as:

$$R_i = \frac{abundance\ of\ rare\ isotope}{abundance\ of\ abundant\ isotope} \tag{2.4}$$

Since the values of the fractionation factors are usually small, the fractionation is expressed as:

$$\epsilon = \alpha - 1 = \frac{R_A}{R_B} - 1 \tag{2.5}$$

Likewise, it is common practice to express the isotopic abundance relative to a standard value. This helps standardise the reported values of the laboratories and offers a clearer tool to evaluate the data. For water, the international standard for $\delta^2 H$ and $\delta^{18} O$ referencing is VSMOW, whose deuterium abundance is R=155.76 ppm [12]. Therefore, the isotopic abundance is expressed using the delta value as:

$$\delta = \frac{R_{sample}}{R_{reference}} - 1 \tag{2.6}$$

A positive delta value means the measured sample is enriched with respect to the reference, while a negative one corresponds to a depleted sample.

2.3 Isotope research and NMR

As was explained in the previous section, isotopic fractionation causes differences in the abundance of isotopes between reservoirs. Therefore, isotopes

can be exploited as a tool to both study the processes undergone by substances and trace their origin. In the case of the latter, once the physical and biogeochemical processes are properly characterised, isotopes can be employed to extract all kinds of information. For instance, carbon isotopes can be used to trace emissions of air pollutants and greenhouse gases, such as CO_2 and CH_4 [13, 14]. Isotopes can also be utilised to study the diets of ancient human civilisations [15]. Other fields of application of isotope research include biology, forensic science, geochemistry, medicine or environmental science [16].

In particular, water isotopes, of which nine stable isotopomers exist, are of great utility in a variety of research fields. Not only can isotopes be used to characterise the water cycle [7], but they find many other areas of interest. For example, in biology, the Doubly Labeled Water method measures energy expenditure of animals and humans by tracing ^2H and ^{18}O water isotopes [17, 18]. Other applications include climate modelling and paleoclimatology, that is, the study of the climate history of the Earth [19, 20].

The use of Nuclear Magnetic Resonance for the study of natural isotope fractionation was first proposed by Martin et al. in 1981 [8], where they analysed the deuterium spectra of a series of ethyl derivatives. In the publication, they showed that NMR could be used to obtain site specific relative concentration values and suggested the use of an external coaxial reference to measure absolute concentration. This led to the creation of the SNIF-NMR (Site-specific Natural Isotope Fractionation NMR) technique [21]. Since then, the field has grown and become of standard use in some areas, such as food authentication. For example, the European Union has adopted SNIF-NMR as their official method to detect the addition of beet sugar to wine[22]. In the past years, advances in measurement precision and processing software have led to the spread of quantitative NMR (q-NMR) [10], which uses the obtained spectra to measure the concentration of chemical species in the solution.

Isotope ratio monitoring by NMR (irm-NMR) was first developed for deuterium. Despite its low sensitivity, one of the advantages of deuterium is that it has a relatively short relaxation time. Currently, irm-NMR is also routinely used for site-specific ^{13}C measurements. The natural variability of ^{13}C is one order of magnitude lower than for deuterium, so it requires a higher precision. In addition, ^{12}C has no nuclear spin and thus produces no NMR signal, so other methods like mass spectrometry or the use of internal reference is required to measure absolute concentration values [23].

Despite having a lower sensitivity compared to Mass Spectrometry, there are several advantages with the NMR approach[2]. First of all, NMR requires minimal sample preparation compared to Mass Spectrometry: samples do not need to be pure, as the various molecules are characterised by different frequency shifts. In addition, it is non-destructive, as samples are recovered and can be analysed several times. In contrast, in Gas Chromatography Isotope Ratio Mass Spectrometry the sample is combusted. Thus, after an NMR measurement samples can be measured again or taken to another experiment.

Moreover, one of the key advantages of NMR is that it gives site-specific information, while IRMS cannot differentiate between isotopomers with same mass. This was one of the breakthroughs highlighted by Martin et al. [21] in their research about NMR spectroscopy applied to isotope research and is one of its main applications today.

As a consequence, NMR has proven to be of great utility for isotope research across many different fields, from medicine [24] to extraterrestrial chemistry [25]. In food science, NMR is well established as one of the techniques to authenticate the origin of food products like vanilla [9] and wine [5], thanks to its ability to offer site-specific information. Furthermore, it also has a variety of applications in environmental sciences, such as tracing the origin of pollutants [6].

In particular, the possibility to obtain site-specific information by NMR analysis has expanded the possibilities of research on the climatic dependence of isotopic parameters. Not only can the origin of a substance be known by its isotopic distribution, but its whole biogeochemical history is now available [26]. Climatic changes between regions (e.g. humidity, latitude, temperature) influence the hydrogen and carbon isotope concentration in water and organic compounds, which can be later used to distinguish the geographical origin of substances.

Chapter 3

Experimental procedure

The preparation, measurement, processing and analysis of all measurements was performed according to the following procedure to guarantee uniformity and reproducibility over all experiments.

First, a beaker was rinsed with water of the corresponding sample type to avoid contamination, and then was filled with the necessary volume of water. Second, the water was introduced in the NMR tube using a pipette. Due to the relatively high sample availability, it was generally not necessary to measure the sample, so tubes were filled to approximately one third of their height. Since the diameter of the NMR tube is narrow, water was slowly and carefully added into the tube to avoid air pockets from getting trapped, which is a hassle to get rid of. Then, tubes were flame sealed to avoid any fractionation that may occur due to evaporation. To do so, first, the remaining water in the end was evaporated, and then the tip of the tube was constantly rotated to guarantee uniform heating. The glass closed inwards by itself, and when it was fully sealed and no air line was visible, it was gradually cooled down to reduce the stress on the glass. Finally, each sample was labelled. For each sample, clean beakers and pipettes were utilised to avoid inter-sample contamination.

The samples measured were the isotopically well-known reference waters from the Centre for Isotope Research, Groningen, labelled GS42, GS46, GS48, GS49, GS53 and BEW09. GS42 and GS46 were precipitation water from the Greenland and Antartic icecap, respectively. GS48 was demineralised Groningen tap water, GS49 distilled ocean water, GS53 tap water from Kangerlussuaq, Greenland, and BEW09 demineralised Groningen tap water with a small addition of water highly enriched in ^{18}O and ^{2}H. Additionally,

another water sample was discussed in the research, BAR2. It corresponds to highly enriched demineralised Groningen tap water (IAEA607 on [27]). The ^{18}O and ^{2}H delta values (expressed on the VSMOW-SLAP scale) of each sample are specified in Table 3.1.

Water Sample	δ^2H	$\delta^{18}O$
GS42	-186.6	-24.5
GS46	-346.0	-43.5
GS49	2.7	0.4
GS53	-113.3	-12.6
BEW09	446.5	55.4
GS48	-43.2	-6.5
BAR2	802.4	99.0

Table 3.1: Isotopic ratios of water samples.

Samples were then taken to the NMR facility and the outer surface of the tubes was cleaned before being placed in the machine. The NMR machine is a Bruker Avance NEO 600 MHz equipped with a Bruker Smart probe.

For each tube, proton and deuterium spectra were measured. The machine performed all measurements of each tube before passing to the next. All the tubes were measured one after the other, with no interruptions in between, unless stated otherwise.

The configuration of the NMR machine for each measurement was the following. No locking was applied since there was only one peak and thus no reference signal to lock to. Shimming was applied on H_2O. For proton measurement, a 30-degree pulse was applied. For deuterium measurement, a 90-degree pulse was applied since the signal was weaker. The other relevant parameters are summarized in Table 3.2. Measurement times were 252 seconds for the proton spectrum and 1016 seconds for deuterium.

Measured data was imported into the NMR software MestReNova 12. The .fid file was automatically transformed into the frequency domain. For the processing of the spectra, first the baseline was automatically corrected. Then, zero filling was applied, increasing the number of points from 64K to 128K. Finally, the phase was corrected manually. A peak with a good phase was considered as symmetric in both sides, with no part of the peak having negative values. A more detailed explanaition can be found in appendix A.

Manual phase correction was found to be one of the most sensitive steps

		Proton	Deuterium
NS	Number of scans	16	32
D1	Relaxation time (s)	10	5
RG	Receiver gain	2.8	101
DS	Dummy scans	2	2
SW	Spectral window (ppm)	14	14
TD	Number of acquired points	65536	5262
O1P	Carrier frequency (ppm)	4.7	4.7
AU	Automation program	au_zgonly	au_zgonly

Table 3.2: Relevant parameters of the NMR experiment configuration.

with respect to the final peak area obtained. Thus, special attention was given to this aspect. After adjusting the phase during the first round of processing, once the integration was performed, the phase was manually adjusted again. During this second round, the superimposed integral curve was used as a qualitative visual reference, since, ideally, the extremes of the curve should be flat. This modified the values of the computed peak area, and was used as a double-proof to try to reduce the human error inherent to the manual phase correction.

Regarding the analysis of the peaks, MestReNova includes an Automatic Peak Picking option, which selects all the peaks in the spectrum and provides information about them, including peak position, intensity, full width at half maximum (width) and area, among others. This algorithm is based on GSD (Global Spectral Deconvolution), renders enhanced resolution and identifies overlapped peaks [28]. An example of its application is shown in Figure 3.1.

The Automatic Peak Picking option returned a value of the area of the peak. However, it was decided to perform the integration manually, since this gave more control over the integration limits. In addition, in the cases where the peak was not well defined, the automatically detected peaks did not match accurately to the peak in the spectra, usually reporting shorter and wider peaks.

Therefore, for manual integration the integration limits were defined as a function of full peak width at half maximum to ensure some uniformity over the spectra. According to [29], an integration width of 25 times the width of the peak covered 99% of the area of the peak. In the case of water, only one peak appeared in the spectrum, so there was no risk of integrals overlapping

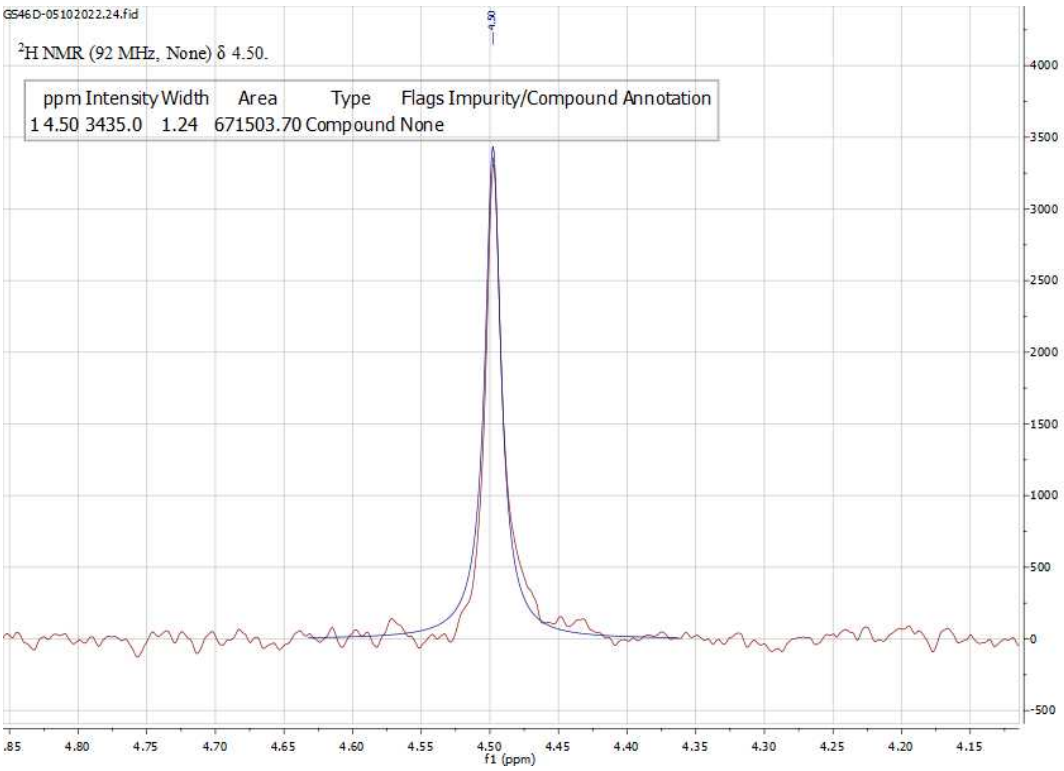

Figure 3.1: Example of processed peak with Peak Picking information. The blue line is the peak detected by Automatic Peak Picking.

each other. An initial analysis of the sensitivity to integration width was completed. Unless stated otherwise, the integration limits were chosen as 35 times the width of the peak to ensure the inclusion of most of the peak area.

These area values were then divided, giving a deuterium-to-proton ratio for each sample. It is important to note that the deuterium and proton peaks belonged to different spectra, and thus, to different measurements. As a consequence, the magnetic field may have drifted between measurements, introducing some error in the calculation of the deuterium to proton ratios. Afterwards, delta values were computed from the ratios with respect to a chosen reference value, and then they were calibrated with the expected results. A 2-point calibration approach was preferred over a 1-point calibration.

For the experiments performed later, a Python code was written with the purpose of optimising and accelerating the analysis of the data. Thus, the integration of the peaks was performed using this Python code.

The code can be employed once the data has been processed and corrected. First, the spectra are combined by selecting them and stacking them using the "Stack items" options in MestReNova. Then, the file can be saved as an NMR CSV file under text format, which contains all the information about the values of the spectra at every point. A second file, containing peak information, such as peak position and width, is needed for the code. This file can be created by first selecting the peaks with the "Peak-picking" tool and then saving the file as an NMR 1D Peak list text file.

The code imports the spectra and peak file and returns a file with the integrated areas for every peak in the peak file. Further input parameters include magnetic field strength, which has to be adjusted to differentiate between proton and deuterium, and integration width factor, which determines the integration limits in relation to the peak width. The area file is created as a text file which can then be copied into an Excel sheet or desired working program, and includes information about spectrum file name, peak position and peak area. In the case of spectra with multiple peaks, all peaks included in the NMR 1D Peak list text file are integrated and reported in the created area file.

This code was tested by comparing the area values returned with the ones obtained manually for a set of measured spectra. The relative error was in all cases under 4% and on average had values under 1%. Thus, it was concluded that the code worked properly.

Chapter 4

Results and discussion

4.1 Initial experiments

The initial idea for the experiments was measuring the deuterium and proton spectra of the sample. Then, their integrated peak areas, which are proportional to the number of nuclei producing the signal, would be used to compute the isotopic ratio of each sample, which would later be calibrated to their expected values.

A total of six samples were prepared, corresponding to water types: GS42, GS46, GS49, GS53 (x2) and BEW09. GS53 was doubled for reproducibility and error testing. The samples were measured three times following the specified configuration, each round of measurements on a different day. The results were then processed and analysed.

For each water type, the deuterium to proton ratios were averaged. The ratios showed an average relative standard deviation of 3%. Later, delta values were computed and calibrated with the two extreme points, BEW09 and GS46. The results are shown in Table 4.1. As can be observed, GS49 was an outlier, with a deviation over 100 permille. Excluding this case, the other three samples showed better results, with average deviation from their expected value of 24 permille. However, these results were far from the desired precision of below five permille.

One of the considered explanations for the observed deviations was contamination during handling of the samples. This was a plausible option as the water beakers were exposed to air during a short time while the tubes were being prepared and filled. For instance, evaporation favours lighter

Sample	Std. Deviation of Deltas (‰)	Expected delta (‰)	Calibrated delta (‰)	Deviation from expected (‰)	Error in the mean (‰)
BEW09	12	446.5	446.5	-	7
GS42	21	-186.6	-211.5	-24.9	12
GS46	24	-346.0	-346.0	-	14
GS49	30	2.7	133.9	131.2	17
GS53	50	-113.3	-139.4	-26.1	30
GS53(2)	40	-113.3	-135.5	-22.2	30

Table 4.1: Results of initial experiments. The second column corresponds to the standard deviation of the three delta values for each sample. The fifth column shows the difference between the expected and calibrated values. BEW09 and GS46 were used as calibration points. GS53(2) corresponds to the duplicated GS53 sample.

molecules, which would increase the deuterium concentration of the sample. Other processes could also have contaminated the samples, even though the beakers were previously cleaned.

In order to test this idea, the isotopic concentrations of the water samples from the NMR tubes were remeasured using the standard CIO equipment. Tubes were opened by heating them with a flame torch, and the water was extracted with a pipette and transferred into small bottles, that were analysed using the Liquid Water Isotope Analyzer (LWIA) manufactured by Los Gatos Research (LGR). The LWIA measures the optical absorbance, which is proportional to the number density of the absorbing molecule. Each isotopologue produces a distinct peak, which allows to measure the abundance of each one selectively and accurately.

The results obtained were in good agreement with the nominal values of the water types, discarding the possibility of sample contamination. Thus, the deviation had to be caused by factors related to the NMR measurement or the processing of the data.

In order to compare the results with a wider set of values, the previous measurements were combined with the data obtained by Prof. Dr. Harro Meijer and Dr. Johan Kemmink during a pilot study in 2021. This set of data was composed of measurements of six different water types: BAR2, BEW09,

GS42, GS46, GS48, GS49 and GS53. In that initial measurement, the NMR tubes were not flame-sealed. Each sample was measured three times.

The deuterium to proton peak area ratios obtained for the second set were significantly different from the first one. This was attributed to a different configuration of the experimental parameters and data processing. Therefore, instead of averaging the ratios of each water type all together, delta values were computed separately for each set of samples with respect to GS42 of the corresponding set. Then, the delta values were averaged, combining both sets, and calibrated with respect to BEW09 and GS46, the same two samples as in the previous analysis. One of the measurements of GS46 from the second set was excluded since it deviated over 100 permille with respect to the delta value of the average of its trio of measurements and was considered an outlier.

Sample	Expected delta (‰)	Calibrated delta (‰)	Deviation (‰)
BEW09	446.5	446.5	-
GS42	-186.6	-188.9	-2.3
GS46	-346.0	-346.0	-
GS49	2.7	112.6	109.9
GS53	-113.3	-113.8	-0.5
GS53(2)	-113.3	-111.9	1.4
BAR2	802.4	789.1	-13.3
GS48	-43.2	-8.2	35.0

Table 4.2: Results combining the initial experiments with those of H. A. J. Meijer and J. Kemmink. The fourth column shows the difference between the expected and calibrated values. BEW09 and GS46 were used as calibration points. GS53(2) corresponds to the duplicated GS53 sample.

The deviation of the calibrated results from the expected values is shown in Table 4.2. GS42 and both GS53 samples display a satisfactory precision. BAR2 and GS48 deviate between 10 and 35 permille points, in absolute values. However, these two samples were only measured in this older experiment and not under the current research measurements. Consequently, the the number of measurements was smaller, which could explain the divergence.

GS49 consistently remained an outlier with the highest deviation. However, the possibility of sample contamination was discarded. Not only was the deviation consistent between the two independent sets of measurements,

but one of the samples was also measured by the LWIA and was proved to have its nominal isotope concentration. The only difference between GS49 and the rest of water types was that it was originally obtained from distilled sea water. In contrast, the other water types originated from tap water or precipitation.

Thus, a chemical analysis of the composition of GS49 was commissioned in order to explore whether some trace elements were still present in the sample and could have modified the NMR signal in any way. The results showed that it contained detectable quantities of Na, K, Ca and Mg, about 10% of the original concentration. On the other hand, GS48, which was also analysed, had no concentrations over the detection limit. It was thus concluded that the distillation process of GS49 had not been very accurate, resulting in the presence of these trace elements. We believe that this could have had some impact on the proton NMR signal, but the extent of this is unclear, so future research could explore this possibility.

Continuing with the analysis of the spread of the measurements, the delta value of each measured deuterium-to-proton ratio was computed with respect to the average ratio of its corresponding water type. This would illustrate how much the measurements for each water type deviated from each other and how reproducible they were. It is important to note that these averages were computed separately for data corresponding to different sets of samples, resulting . The average deviation was of 22 permille points, but there were several values over 50 permille. This pointed towards a lack of reproducibility of the measurements, which could be related to the drift of the magnetic field. Furthermore, this deviation was higher than the desired value for reproducible results and thus required further improvements on the measurement and processing method.

4.1.1 Reproducibility

A decision was made to perform an experiment to study the drift of the magnetic field and reproducibility of the measurements. If a trend were to be observed, it could be used to correct the results or modify the measuring order by, for example, intercalating the reference with the unknown samples.

However, this last possibility came into conflict with the working procedure of the NMR facility. Unlike others, the NMR facility at RUG is under a multi-user environment shared among researchers of various fields and, thus, is not exclusively dedicated to one specific use. Once the samples are placed

and measurements programmed, the algorithm of the machine decides its own order, taking into account a priority list among other factors. Thus, programming all measurements at the same time does not guarantee that they will be performed immediately one after the other, which could result in a more pronounced drift. Likewise, it is not possible to program a measuring scheme which intercalates several samples. In contrast, once one sample is inserted into the NMR, all the scheduled measurements are performed. Therefore, if, for instance, one was to measure the reference before every new sample, each reference and sample measurement pair would have to be uploaded separately once the previous pair was successfully analysed. This further complicates the working procedure. Nevertheless, it is important to underline that during this research, every set of measurements was completed one after the other unless otherwise stated.

Thus, the sample containing GS42 water was measured 15 times following the same procedure as for the previous experiments in order to study the reproducibility of the measurements and drift of the magnetic field.

The integrated results were then analysed. The area of the deuterium and proton peak had a relative standard deviation of 8% and 1.4%, respectively. The higher deviation in the deuterium peak was attributed to the lower signal to noise ratio. After that, delta values of the samples were computed with respect to the average deuterium to proton ratio measured. The results are plotted in Figure 4.1. As it can be observed, the spread of the results was significant. The standard deviation was 80 permille, with some measurements showing a >100‰deviation. In addition, they did not seem to follow any clear trend as a function of measurement number.

Several different integration widths were tested in order to find the value that resulted in the lower spread. Integration limits ranging from 1 to 40 times the peak width with jumps of five were evaluated, for proton and deuterium separately. In the case of deuterium, the spread decreased with integration width, from over 8% to 1.8% relative standard deviation for the smallest integration limit. This could be because, for larger limits, the noise signal introduced a higher variability. In contrast, for the proton area, the spread reached a minimum for integration limits of 10 times the peak width, and then increased for smaller values. However, the improvement here was not as pronounced as for the previous case. The combination of these two optimal limits, also included in Figure 4.1, resulted in a standard deviation of the delta values with respect to the average of 17 permille.

These results hinted at the use of different integration limits for proton

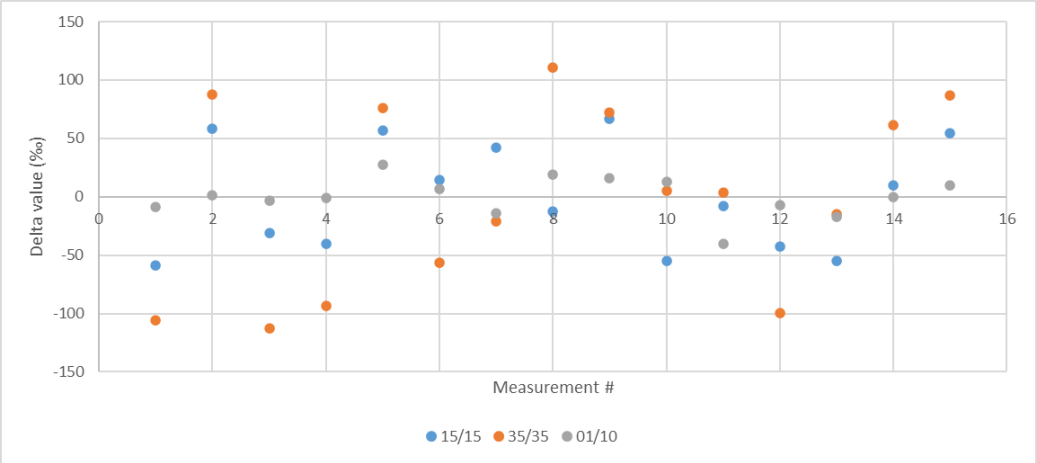

Figure 4.1: Delta values computed with respect to the average deuterium to proton area ratio for the series of measurements of GS42. The names refer to the integration widths of the deuterium and proton peak, respectively. That is, 35/35 corresponds to values obtained by integrating both peaks with limits 35 times their full peak width at half maximum, while 01/10 corresponds to an integration width of 1 and 10 times the peak width for deuterium and proton, respectively.

and deuterium for a better precision, due to the lower signal-to-noise ratio for deuterium. Likewise, it also seemed to suggest that, for deuterium, a smaller integration width than what was previously considered could give better precision results. However, these measurements only corresponded to one sample, and thus should be corroborated by other complementary measurements before any definitive conclusions were to be drawn.

It is unclear what the causes for the lack of reproducibility were. One option could be the drift of the magnetic field between measurements. As it was explained, the frequency of the recorded signal was directly proportional to the magnetic field, so variations on its value would result in a broadened peak. Shimming was performed every time a new sample entered the machine in order to correct for this drift. In this case, since the same sample was measured, this only took place once. In principle, this was the better way of proceeding. Dr. Kemmink contacted Bruker, the manufacturing company, and performed several experiments changing the configuration, without any conclusive results so far at the time of writing.

All in all, these deviation results were higher than what would be desirable for the precision required for isotope abundance research.

4.2 Experiments with internal reference

After concluding that the previous method could not be employed for precise isotope abundance measurements, a search in the literature was conducted in order to find more appropriate procedures. As was found, most experiments include an internal reference in the solution. This way, since the area of the peaks is proportional to the number of nuclei producing the signal, it is sufficient to know the quantity of reference material added in order to compute the quantity of sample material. Mathematically, the concentration x can be expressed as follows:

$$x_i = \frac{A_i}{A_{ref}} \cdot \frac{N_{ref}}{N_i} \cdot \frac{m_{ref}}{m_i} \cdot \frac{M_i}{M_{ref}} \cdot x_{ref} \tag{4.1}$$

Where A are the areas of the peaks of reference and sample, m their masses and M their molar weights. In addition, it is important to include N, the number of sites producing the signal on each molecule of reference and sample.

The inclusion of a reference in the sample would result in a spectrum with two peaks, water and reference. The reference, whose concentration should be known, could then be used to correct any drift in the measurements. That is, if, for instance, changes in the magnetic field caused the peaks to drift between measurements, both the water and reference peaks were expected to drift together, so the latter could be used to correct for that drift.

There are two different ways to include the reference compound in the experiment: external and internal reference. To add an external reference [30], a coaxial tube containing the reference is introduced inside the NMR tube. Nevertheless, this presents some disadvantages, as the sample volume is reduced, which leads to an increase of the measurement time. Likewise, the volumes need to be carefully calibrated, which slows down the process, and the cost of the materials can increase compared with the standard NMR tubes. However, this technique might be necessary when reference and sample should not be mixed.

On the other hand, internal referencing is the method most usually applied [31, 32]. This consists on dissolving a reference compound in the so-

lution to be measured. The chosen internal reference should be soluble in the sample and, ideally, it should not interact with it to avoid modifying the spectrum. Moreover, it should be highly pure and its peak should not overlap with any other peak from the sample. Some commonly used reference compounds include tetramethylurea (TMU) and sodium 3-(trimethylsilyl) propionate (TMSP).

Usually, for deuterium and proton NMR measurements, two different samples are prepared, one for deuterium and one for proton measurement, each one with a different reference. The deuterium reference is often enriched on deuterium with respect to its natural abundance. Then, computing the concentration of deuterium and proton separately leads to the isotopic concentration.

A second approach to this can be found in the research undertaken by Y. Monakhova and B. Diehl [33]. Here, the reference compound was chosen such that it produced a peak both in the proton and deuterium spectra. Thus, measurement of both signals in the same compound can directly lead to the calculation of the isotopic abundance of the analysed material. As was highlighted in the paper, since the same sample is measured for both spectra, the exact values of the molar masses, weights and purities do not influence the result of the isotopic abundance. That is, by being able to measure proton and deuterium in the same tube, any inaccuracies in those parameters would automatically get corrected when the ratio is taken, as both spectra would correspond to the same number of molecules of reference and sample. In contrast, the only source of error stems from the integration of the peaks. Thus, if an appropriate reference can be found, this technique provides a clear advantage.

After an initial failed attempt with sodium trimethylsilylpropanesulfonate (DSS), it was decided to prepare a reference sample with a known isotopic concentration starting from two fully protonated and deuterated samples. The compound chosen was acetonitrile (CH_3CN), which is soluble in water, has one type of proton and whose deuterated version (CD_3CN) is available commercially and is used as an NMR solvent.

A 100 mL bottle of CH_3CN (271004-100mL) with 99.99% purity and ten 0.6 mL ampoules of CD_3CN (151807-10x0.6mL, Merck) with $\geq$99.8 atom % D purity were purchased for the experiment. In order to acquire the desired precision in the concentration of the mixture, each component was weighed. The mass of deuterated acetonitrile was 0.39456 grams and it was mixed with 23.12014 grams of its protonated counterpart. The isotopic abundance

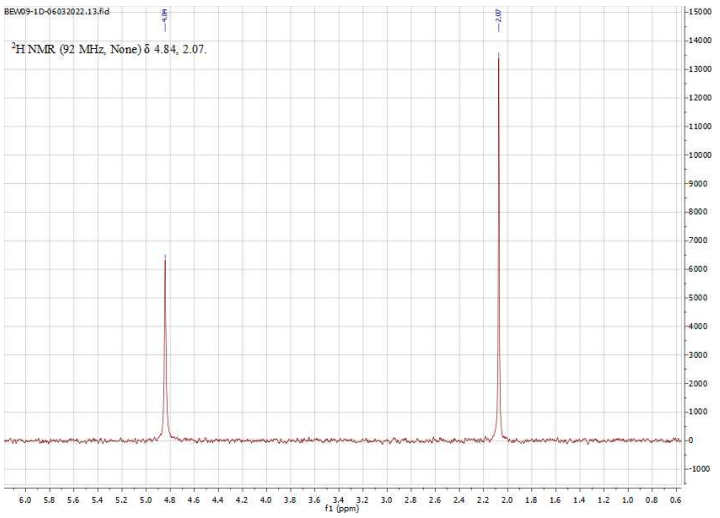

(a) Deuterium spectrum for BEW09 with acetonitrile

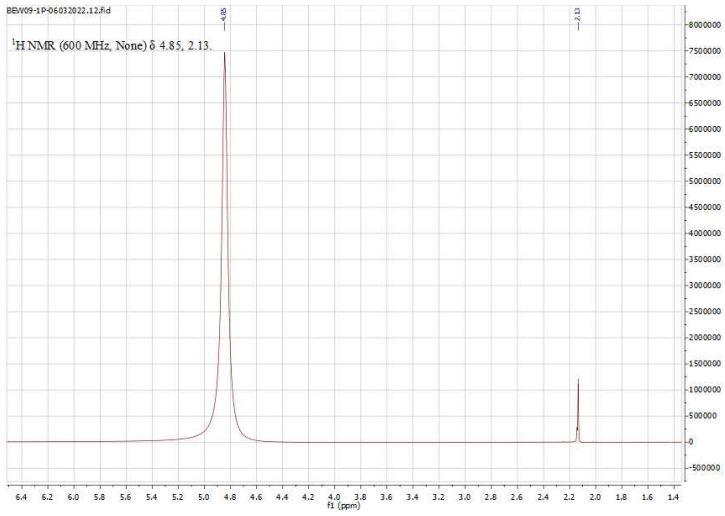

(b) Proton spectrum for BEW09 with acetonitrile

Figure 4.2: Deuterium and proton NMR spectra of BEW09 with acetonitrile. The reference concentration is specified in section 4.2. The peak in the left corresponds to water and the peak in the right to acetonitrile.

of deuterium in the reference sample was then 0.01597. Then, 0.02 mL of reference were added to 0.6 mL of the water sample. Since acetonitrile has a low boiling point, tubes were sealed with a cap instead of melting the open

end. Nine samples were prepared, corresponding to BEW09, GS42 and GS46, each repeated three times.

With this isotopic ratio and concentration for the reference, a peak for deuterium and proton were expected in a range of two orders of magnitude from the water peak. The deuterium peak was expected to be higher than water, which would guarantee its measurement above the baseline noise, while the proton peak was expected to be smaller than water but still significantly higher than the noise signal. The samples were measured following the same protocol and NMR spectra were obtained. In Figure 4.2, example spectra are shown for both deuterium and proton. The peaks for water and acetonitrile can be distinctly identified.

The idea for the analysis was to use the reference peak to correct for the drift in the experiment, as both peaks would drift together with the changes in the magnetic field. Thus, dividing the areas of both peaks would normalise the deuterium peak and correct the inhomogeneities. However, this did not work as expected. Using the reference peak to normalise the areas did not improve significantly the obtained results. Moreover, the peak area values did not follow the same trends for water and reference.

The normalised results for the ratio were then calibrated using the average delta value of the two extreme water types (BEW09 and GS46). The results are shown in Table 4.3. Deviations for the final delta values were under 50 permille, and had an average of around 16‰. This was not a significant improvement compared with the results obtained without the reference.

The reason for this was not fully clarified. One of the possible explanations might be related with the added difficulty of correcting the phase of two peaks. Using the MestReNova software, manual correction could be applied for both peaks separately. Left clicking and dragging in the manual correction panel corrected the highest peak, while right clicking corrected the lower peak. However, the corrections could not be performed as accurately as in the previous spectra.

Another important factor to take into account was that the proton peaks of acetonitrile were not well defined. Some had very pronounced shoulders and others even appeared as doublets. It is unclear what could have caused this since there was no consistency among the measured spectra. A possible explanation could be related to poor shimming of the magnetic field or the processing of the data, particularly the manual phase correction. As an example, Figure 4.3 shows two measured proton peaks of acetonitrile.

Sample	Expected delta (‰)	Calibrated delta (‰)	Deviation (‰)
BEW09 #1	446.5	470.8	-24.3
BEW09 #2	446.5	435.1	11.4
BEW09 #3	446.5	433.6	12.9
GS42 #1	-186.6	-234.2	47.6
GS42 #2	-186.6	-204.3	17.7
GS42 #3	-186.6	-182.3	-4.3
GS46 #1	-346.0	-359.2	13.2
GS46 #2	-346.0	-332.6	-13.4
GS46 #3	-346.0	-346.2	0.2

Table 4.3: Deviation of the delta values computed with the the acetonitrile reference. Calibration was performed with respect to the average value of BEW09 and GS46. Integration limits were taken as 35 times peak width for proton spectra and 5 times peak width for deuterium spectra.

4.2.1 Reproducibility

Intending to further study the possible improvements introduced by the addition of the reference, the reproducibility of the experiment was studied. To do so, one of the samples corresponding to GS42 was measured nine consecutive times. The spectra were then processed and analysed. In this case, the automatic phase correction tool was employed to correct the proton spectra.

Several integration limits, ranging from 1 to 40 times the peak width with steps of 5, were tested in order to analyse how the deviation depended on it. The spread of the water deuterium peak area decreased from 9% for a factor of 40 to 2% for a factor of 5, and in the case of the reference deuterium peak it decreased from 3% to 1% for the same factors. In both cases, integrating only over the peak width resulted in a small increase of the spread.

In the case of proton, it followed the opposite trend. The spread decreased for increasing integration area, from 0.5% for a factor of 5 to 0.4% for a factor of 40 in the case of water, and didn't change significantly in case of the reference peak. However, the improvement was not as pronounced as with deuterium, so results were not as conclusive.

In light of these results, and taking into account those from section 4.1.1, a difference in the behaviour of the deuterium and proton integrals could be inferred. For the proton peak, higher integration widths seemed to result

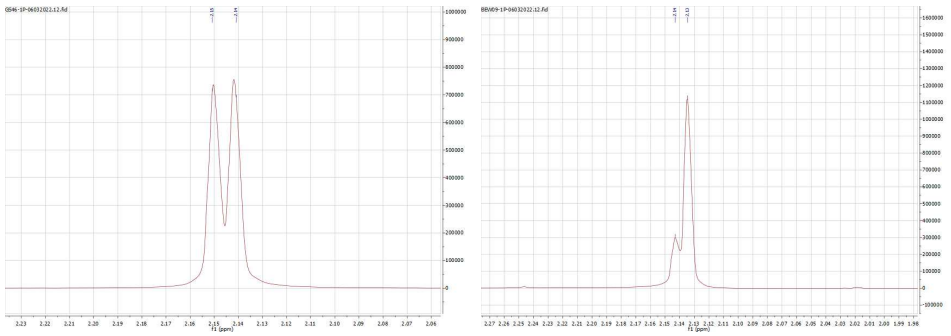

(a) Acetonitrile peak in GS46. (b) Acetonitrile peak in BEW09.

Figure 4.3: Two examples of not well defined proton peaks of acetonitrile. Figure 4.3a corresponds to a GS46 spectrum and Figure 4.3b to BEW09.

in a more compact set of values, which could be due to the inclusion of a higher proportion of the total area of the peak. In contrast, for the deuterium peak, the spread was minimised for the shorter integration widths. This was attributed to the lower signal to noise ratio, which meant that wider limits included more noise, which induced a higher variability of the data.

Furthermore, using the reference peaks to correct for the drift in the water peaks did not seem to work. In fact, the additional fluctuations introduced by the reference peak resulted in less precise average ratios for the peak areas. In all cases, not normalising by the reference peak translated into final deuterium to proton ratios with a lower standard deviation. To illustrate this point, Figure 4.4 shows the relative deviation from their average value of the peak areas for water and reference peaks, and for the normalised value. As can be observed, both compounds did not follow the same trend, and the normalised value did not always improve the deviation of the measured value.

The delta values were computed with respect to the average value of the normalised ratio, which would give a measure of how reproducible the experiment was. Taking the integration widths that resulted in the less spread peak areas, a factor of 5 for deuterium and 40 for proton, the average delta value was 30 permille points.

Thus, it was concluded the inclusion of the reference compound did not improve the reproducibility of the experiment. The reason why it did not work is unknown and actually hard to understand.

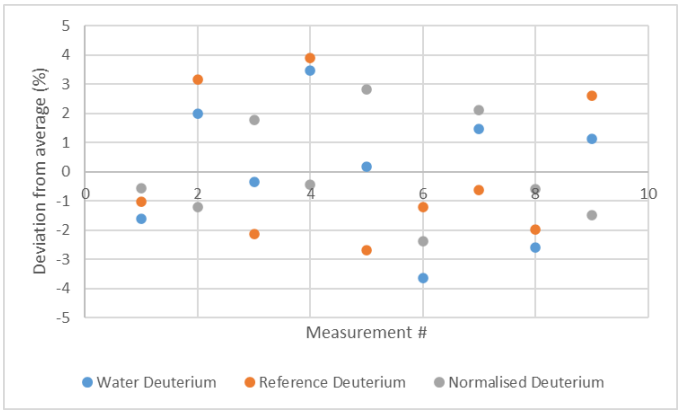

(a) Deuterium

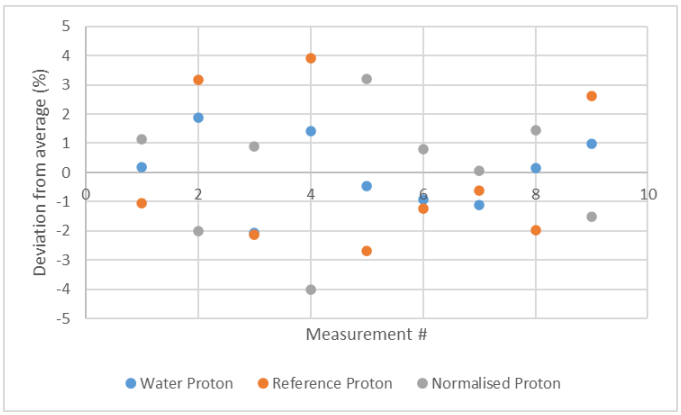

(b) Proton

Figure 4.4: Relative deviation from the average value of the peak area. Figure 4.4a corresponds to deuterium and Figure 4.4b to proton. Each image differentiates between water and acetonitrile peak, and also includes the normalised value obtained by dividing the water by the acetonitrile value.

4.3 Last measurements and future developments

During the last weeks of the research, different measurement sequences were tested to explore in which manner the previous results could be improved. Two main modifications were introduced upon the original working procedure which seemed to translate into better results.

First, once the sample was introduced in the NMR machine, a waiting time was added before the first measurement started. This was because the room temperature was 20^{o}C, while the experiment temperature was 25^{o}C. As a consequence, when the sample was first inserted in the machine, it was not in thermal equilibrium, which could induce some instabilities in the measurement, as was suggested by Dr. Kemmink. The time for sample equilibration was included in the experiment by writing the command "aftersec" before the LOCK-OFF command. In particular, a waiting time of 20 minutes was added, that is, "aftersec 1200; LOCK-OFF".

This change seemed to improve the results of the first measurement. Initially, the first data point was one of the most deviated points from the average. However, once this modification was included, the spread of this first point was reduced, resulting in a more compact set of measurements. A comparison of measurements with and without waiting time is shown in Figure 4.5. These points correspond to the peak area value of deuterium peaks in one of the GS42 samples with acetonitrile reference compound previously used in 4.2. As can be seen, without waiting for thermal equilibration, the first measured value was significantly deviated from the rest, both for water and acetonitrile.

The second modification was related to the sequence of the proton and deuterium measurements. In the original working procedure, proton and deuterium spectra were obtained alternately, that is, proton, deuterium, proton, deuterium and so on. The reasoning behind it was that this way back-to-back proton and deuterium measurements could be used to compute the isotopic ratio and the influence of the magnetic field drift over time could be reduced.

In contrast, a second procedure was tested where all deuterium measurements were obtained first and later all proton measurements were performed. This was expected to increase the stability of the obtained peaks as the configuration of the machine did not have to be modified for every new measurement, as, for example, deuterium and proton require different magnetic field strengths.

The results of this change were not as clear as those of the previous one, as it was not studied separately. Nevertheless, since the combination of the two mentioned modifications seemed to decrease the spread of the areas, both were implemented in the final experiments.

Thus, the samples containing BEW09, GS42, GS46 and acetonitrile, with the concentrations specified in section 4.2, were measured. For BEW09 and GS46, one sample was measured, while for GS42 two tubes were measured

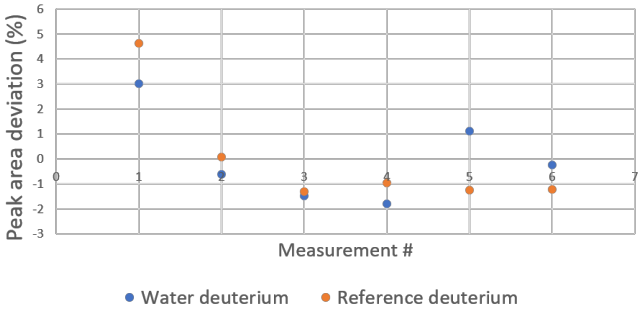

(a) Without waiting time

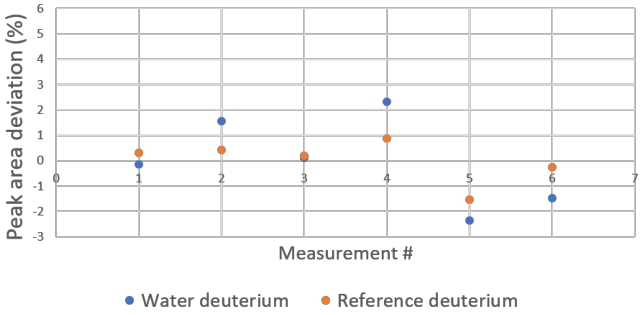

(b) With waiting time

Figure 4.5: Deuterium peak area relative deviations from average for integral limits corresponding to the peak width. Figure 4.5a are values obtained without waiting for the first measurement when the sample is introduced. Figure 4.5b are values obtained after waiting for twenty minutes for the first measurement.

as a reproducibility test. In addition, two new samples were prepared, containing GS48 and GS53. This was done following the same procedure as for the previous ones and with the same concentration of the same acetonitrile. After waiting 20 minutes inside the NMR spectrometer, deuterium was measured six times. Then, after waiting for 5 minutes, proton was measured three times. The second waiting time was smaller since the sample had already been equilibrated, and the number of measurements was lower as the spread of the proton peak area had been observed to be smaller than that of deuterium, so less measurements were necessary for precise peak area values.

Regarding the processing and analysis of the data, the only difference relied on the fact that different areas were used for deuterium and proton. This

was motivated by the findings of the previous experiments, where smaller integration limits for deuterium significantly reduced the spread of the peak area values, while for proton wider areas tended to result in less deviated values. Thus, for deuterium, the integral limits were taken as 5 times the peak width, while for proton they were taken as 40 times the peak width.

For each water type, deuterium to proton ratios were computed separately. Then, delta values with respect to one reference ratio of GS42 were computed. Afterwards, those deltas were calibrated using the average delta value of BEW09 and GS46. Finally, the six calibrated deltas of each water type were averaged and the deviation from the expected value was computed. Two points, belonging to GS46 and GS53 were not included in the analysis since they were significantly more deviated than the others of their group.

Sample	Expected delta (‰)	Average calibrated delta (‰)	Standard Deviation (‰)	Deviation from expected (‰)	Error in the mean (‰)
BEW09	446.5	446.5	30	-	12
GS42	-186.6	-191.2	18	4.6	7
GS46	-346.0	-346.0	13	-	6
GS42(2)	-186.6	-190.1	13	3.5	5
GS48	-43.2	-52.0	40	8.8	15
GS53	-113.3	-109.8	11	-3.5	5

Table 4.4: Average calibrated delta, standard deviation of average delta, deviation from expected value and error in the mean, following the experiment configuration of 4.3, where six delta values were obtained for each sample. For GS42, the first data point was lost due to a problem in the NMR interface. For GS46 and GS53 one data point was not taken into account as they were considered outliers. The final column corresponds to the error in the mean when averaging the individual calibrated deltas for each water type. BEW09 and GS46 were used to calibrate the results.

The results are summarised in Table 4.4. As can be observed, the obtained values were the best results of the project with respect to their accuracy, as three out of four samples deviated less than 5‰from the expected value. The fourth, GS48, deviated still less than 10‰, which was an improvement compared to previous experiments. However, the spread of the individual measurements, although an improvement in some cases, was still significant.

The standard deviations of calibrated delta values ranged from 11 to almost 40‰. The sample having the highest standard deviation also corresponded to the one with the highest deviation from the expected value, which might indicate some kind of problem with the sample. This could be related to the preparation of the tube, the experiment or the processing of the data, although it could also be just a statistical fluctuation.

Overall, this alternative working procedure did seem like an improvement over the initial experiments, as the accuracy of the final results was increased to satisfactory levels in all but one case. The precision was also augmented but not to the same degree. Thus, introducing a waiting time for thermal equilibrium before the first measurement and measuring deuterium and proton separately instead of alternately seemed to be the better option for future experiments.

Nevertheless, before any definitive conclusions can be drawn, a larger sample size and set of measurements is needed. Moreover, future feedback from BRUKER, the manufacturing company of the NMR machine, about the optimal configuration of the NMR could translate into more precise peak areas. Likewise, the results of the analysis of the GS49 analysis seemed to suggest that the purity of the sample and presence of trace elements could influence the proton NMR signal, so more research should be conducted on this topic to understand the possible mechanisms behind it, as well as the extent of its effect.

Finally, future research could focus on ways to reduce the spread of the obtained average values, possibly through a better processing of the data. An option that could be explored would be the use of deuterium peak height instead of peak area [34]. This could further improve the precision, due to the lower signal-to-noise ratio for deuterium and the observed rise in precision with lower integration limits. However, this possibility requires very well shimmed spectra since height is dependent on peak shape. Therefore, improvements on the experimental and processing part could be explored to account for this. Of course, increasing the measurement time, either by longer integration time or simply more measurements epr sample, would also increase the precision, but at the cost of longer processing times.

Chapter 5

Conclusion

In this project the use of Nuclear Magnetic Resonance for the quantitative measurement of deuterium water isotopes at the University of Groningen has been studied. To do so, different experimental configurations as well as data processing options were tested, with the following results.

On the one hand, from an experimental point of view, it was found that it is important to introduce a waiting time before the first measurement to allow for the sample to reach thermal equilibrium, as the temperature inside and outside the spectrometer was not the same.

In addition, the measured spectra were found to be very sensitive to the stability of the magnetic field. Therefore, measuring deuterium and proton spectra separately instead of alternately seemed to be a better option, as this was believed to reduce the possible fluctuations in the magnetic field derived from the change between configurations for proton and deuterium. Further reductions in the inhomogeneities of the magnetic field could be introduced once a reply from the spectrometer manufacturing company is received about the typical experimental configuration.

Likewise, another important aspect to take into account related to the NMR facility was that sequences of measurements could not be programmed. This was a result of the multiuser environment and the priority list under which the spectrometer functions at the University of Groningen. A separate installation for quantitative NMR analysis could solve this issue.

On the other hand, one of the main findings on the data processing side was that using different integration widths for deuterium and proton augmented the precision of the results. In particular, a narrower integration width for deuterium peaks and wider for proton was found to be best, which

was attributed to the lower signal-to-noise ratio in the case of deuterium. Following this idea, one of the suggestions made for future research is exploring the possibility of using deuterium peak intensities instead of areas.

In regards to the experiments with an internal reference, they were not found to improve significantly the precision of the final results. This could be caused by poor shimming of the magnetic field or by the added difficulty of processing two peaks at the same time. However, since this technique is typically used by other laboratories, further research and feedback from other research groups could increase its precision compared to measurements without a reference.

Overall, despite its poor precision, which could be compensated with a larger number of measurements, final results showed a reasonable accuracy. Thus, NMR spectroscopy has the potential to become a useful tool for the Center of Isotope Research with future research and improvement.

Appendix A

Working with MestReNova

In this appendix the processing and analysis of the .fid file obtained in the NMR experiment will be shown, using MestReNova 14 software (Modern version). This is based on [29].

The NMR data is received in a compressed .zip file via email, which can be unzipped. Once the MestReNova program is opened, the extracted folder can be dragged and dropped into a new file. Thus, the data is opened and the NMR spectrum is displayed, as in Figure A.1a.

The spectrum is then processed in the following manner. First, Automatic Baseline Correction is applied. This tool can be found in the Processing window, see Figure A.1b. Second, Zero filling was applied, which increases the number of points before the Fourier transformation was performed on the FID. In Figure A.1c the number of points is increased from 64K to 128K.

Figure A.2a shows how to zoom in. To do so, right click in the spectra, select Zoom In and select the desired part of the spectrum. The height of the peaks can be changed scrolling up and down with the scroll wheel in the mouse.

The last part of the applied processing is correcting the phase. This tool is indicated in Figure A.2b. Left clicking on the blue box corrects the phase of the highest peak, while right clicking corrects the phase of the other peaks (First Order Phase Correction). The blue line indicates the pivot point, whose phase is not modified [28]. A spectrum with corrected peaks is shown in Figure A.2c.

Moving to the analysis of the peaks, Automatic Peak Picking can be found under the Analysis window, see Figure A.3a. Since Automatic Peak Picking sometimes selects peaks from the noise, the Manual Threshold tool is

recommended. In order to view peak information (position, intensity, width, area...), click on NMR Peak Table as in Figure A.3b. The pop-up window can be dragged to the side, where it may be anchored.

Manual integration can be performed by clicking on Manual Integration and drag the mouse to select the area to integrate (Figure A.3c). A second option is to introduce the integration limits manually, which can offer higher precision. This can be done from the Integral Manager window shown in the right of Figure A.4a. In order to show this window, and to control which windows are displayed at all, click on Tables under the View option, as indicated in Figure A.4a. From there, pop-up windows can be managed.

Finally, Figures A.4b and A.4c show how to stack items. When multiple spectra are selected in the left column, a new window will appear, called Stacked. This offers new options to work with many spectra at the same time, including the Stack Items option, which will stack them as in Figure A.4c.

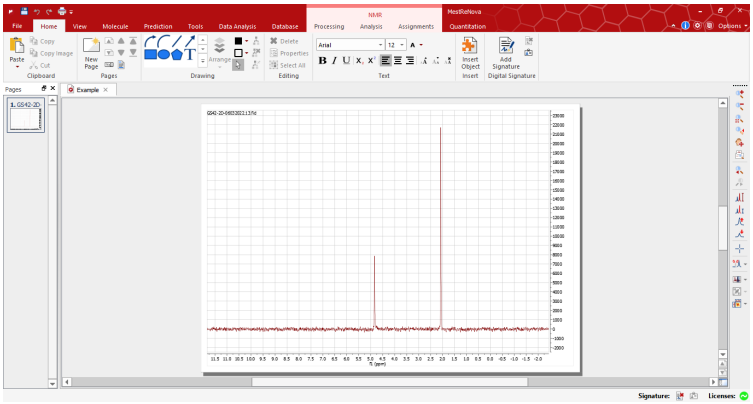

(a) First time opening a file in MestReNova.

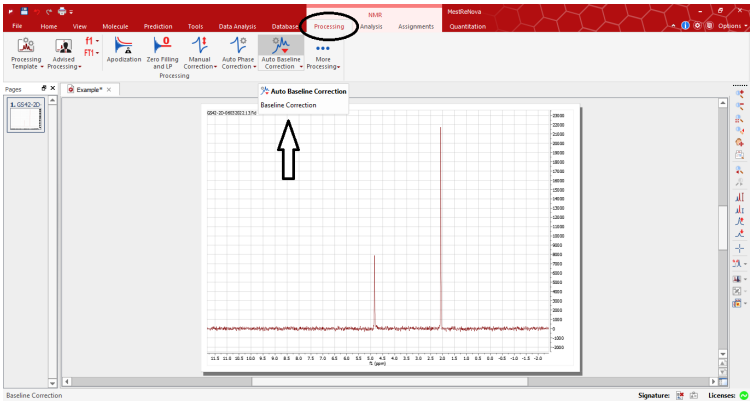

(b) Applying Auto Baseline correction.

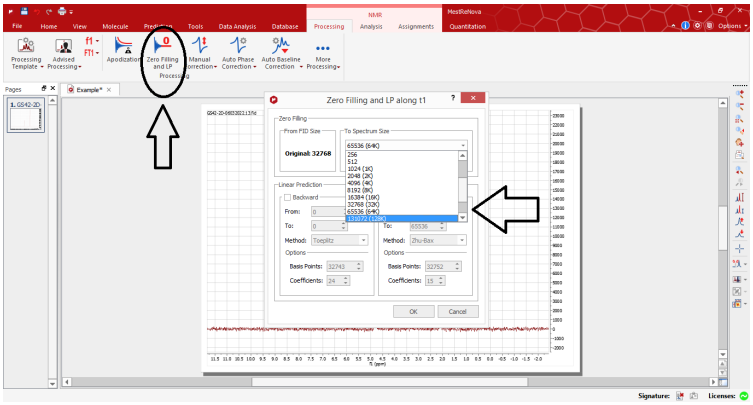

(c) Applying Zero filling: increasing number of points from 64K to 128K.

Figure A.1: Processing with MestReNova: opening file and initial processing.

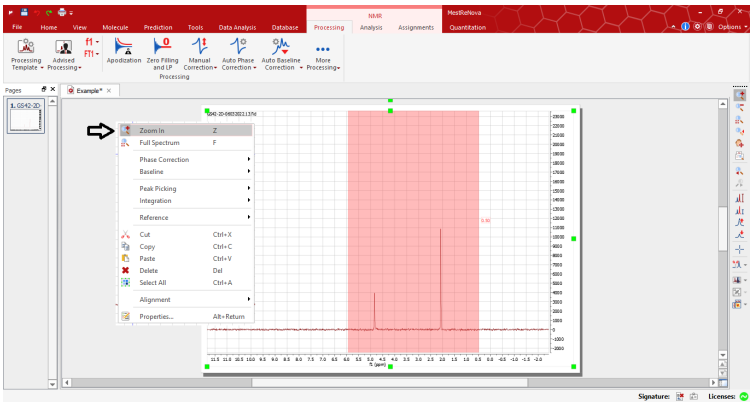

(a) Example of zooming in the spectrum.

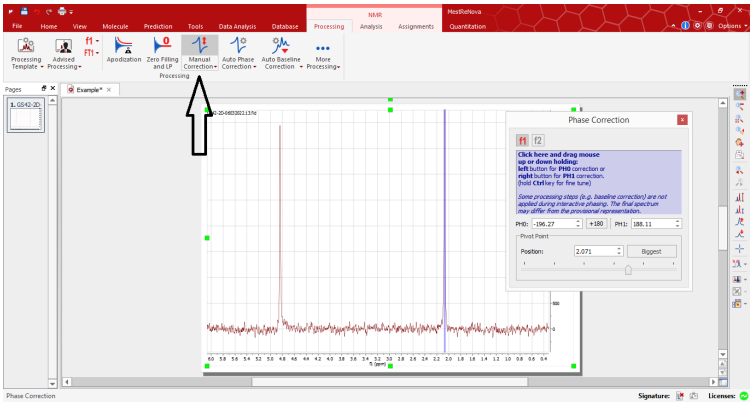

(b) Applying Manual Phase Correction.

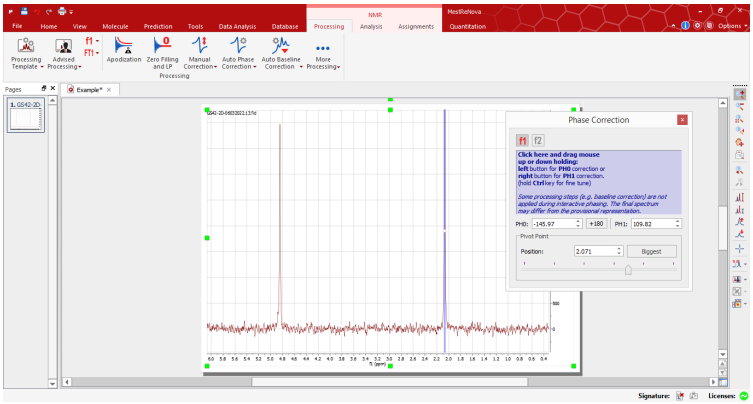

(c) Spectrum after Manual Phase Correction.

Figure A.2: Processing with MestReNova: Manual Phase Correction.

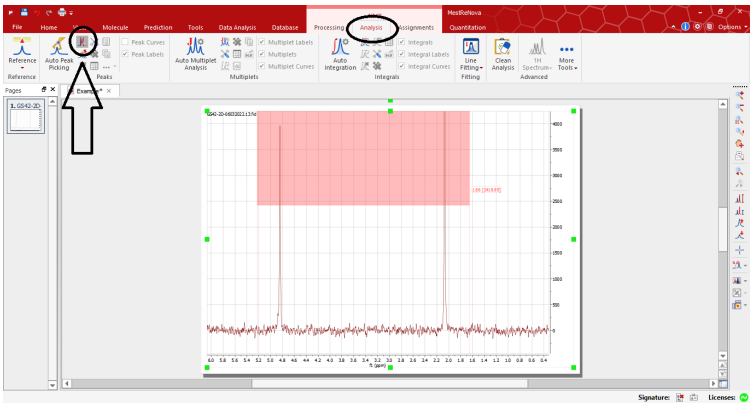

(a) Applying Auto Peak Picking.

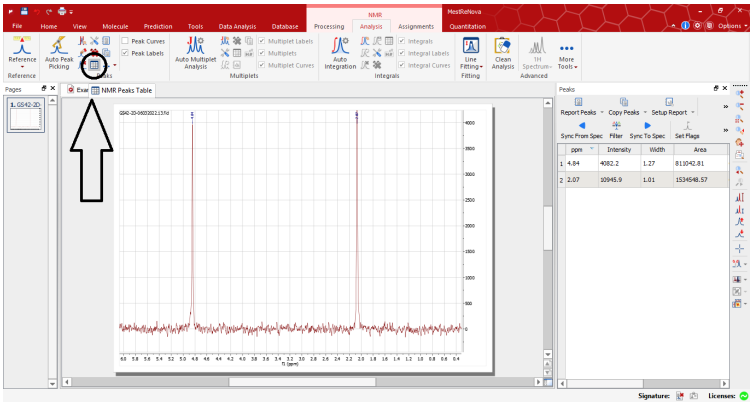

(b) Showing the Peak Table.

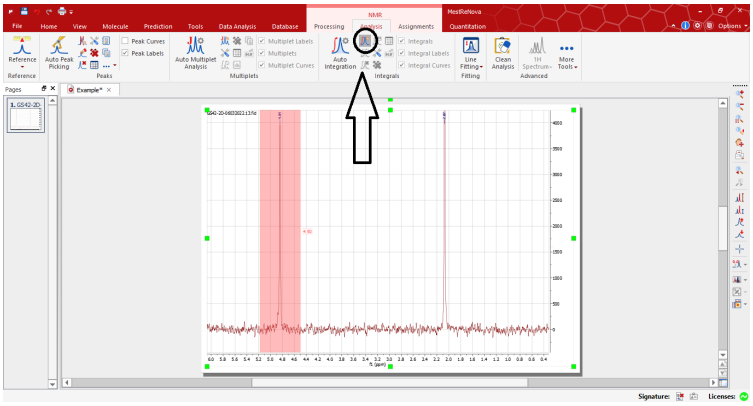

(c) Integrating manually.

Figure A.3: Analysis with MestReNova: Peak picking and integration.

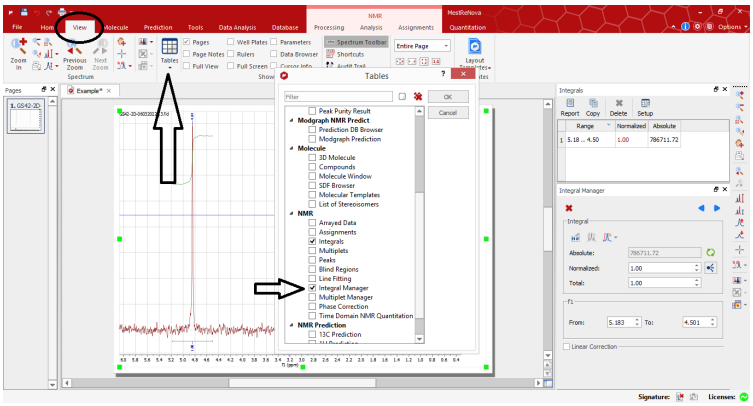

(a) Viewing tables.

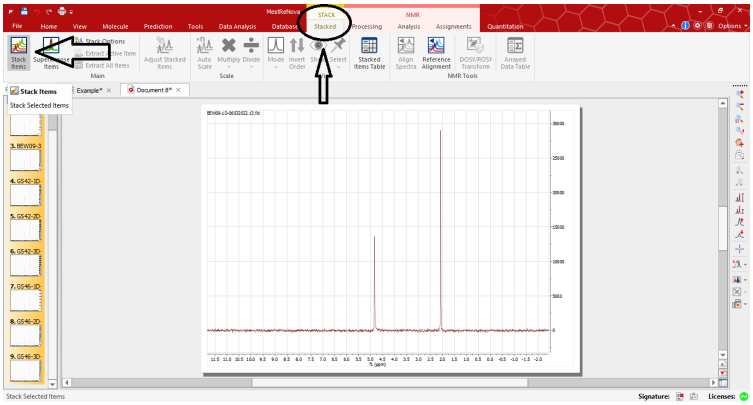

(b) Stacking multiple spectra.

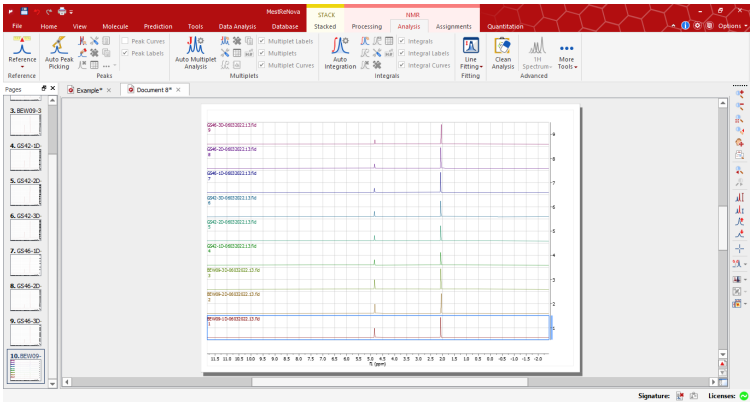

(c) Stacked spectra.

Figure A.4: Analysis with MestReNova: Viewing tables and stacking multiple spectra.

Bibliography

[1] James Keeler. *Understanding NMR spectroscopy*. John Wiley & Sons, 2011.

[2] Abdul-Hamid M Emwas. "The strengths and weaknesses of NMR spectroscopy and mass spectrometry with particular focus on metabolomics research". In: *Metabonomics*. Springer, 2015, pp. 161–193.

[3] WG Mook. "Principles of isotope hydrology. Introductory course on Isotope Hydrology". In: *Dep. Hydrogeol. Geogr. Hydrol., VU Amsterdam, Amsterdam* (1994).

[4] R Mathur-De Vre. "The NMR studies of water in biological systems". In: *Progress in biophysics and molecular biology* 35 (1980), pp. 103–134.

[5] Josep E Giménez-Miralles, Domingo M Salazar, and Isabel Solana. "Regional origin assignment of red wines from Valencia (Spain) by 2H NMR and 13C IRMS stable isotope analysis of fermentative ethanol". In: *Journal of agricultural and food chemistry* 47.7 (1999), pp. 2645–2652.

[6] Jennifer R McKelvie et al. "Quantitative site-specific 2H NMR investigation of MTBE: potential for assessing contaminant sources and fate". In: *Environmental science & technology* 44.3 (2010), pp. 1062–1068.

[7] Jing Zhou et al. "Using stable isotopes as tracer to investigate hydrological condition and estimate water residence time in a plain region, Chengdu, China". In: *Scientific reports* 11.1 (2021), pp. 1–12.

[8] GJ Martin and ML Martin. "Deuterium labelling at the natural abundance level as studied by high field quantitative 2H NMR". In: *Tetrahedron letters* 22.36 (1981), pp. 3525–3528.

[9] Eric Jamin et al. "Determination of Site-Specific (Deuterium/Hydrogen) Ratios in Vanillin by 2H-NuclearMagnetic Resonance Spectrometry: Collaborative Study". In: *Journal of AOAC International* 90.1 (2007), pp. 187–195.

[10] Santosh Kumar Bharti and Raja Roy. "Quantitative 1H NMR spectroscopy". In: *TrAC Trends in Analytical Chemistry* 35 (2012), pp. 5–26.

[11] Gladys H. Fuller. *Standard reference data — NIST*. 1976. URL: `https://srd.nist.gov/JPCRD/jpcrd85.pdf`.

[12] International Atomic Energy Agency (IAEA). *Reference Sheet for International Measurement Standards*. 2006. URL: `https://nucleus.iaea.org/rpst/documents/vsmow_slap.pdf`.

[13] Yiqiang Zeng et al. "Application of gas chromatography-combustion-isotope ratio mass spectrometry to carbon isotopic analysis of methane and carbon monoxide in environmental samples". In: *Analytica chimica acta* 289.2 (1994), pp. 195–204.

[14] Gan Zhang et al. "Radiocarbon isotope technique as a powerful tool in tracking anthropogenic emissions of carbonaceous air pollutants and greenhouse gases: A review". In: *Fundamental Research* 1.3 (2021), pp. 306–316.

[15] Richard P Evershed et al. "Application of isotope ratio monitoring gas chromatography–mass spectrometry to the analysis of organic residues of archaeological origin". In: *Analyst* 119.5 (1994), pp. 909–914.

[16] Eric Lichtfouse. "Compound-specific isotope analysis. Application to archaelogy, biomedical sciences, biosynthesis, environment, extraterrestrial chemistry, food science, forensic science, humic substances, microbiology, organic geochemistry, soil science and sport". In: *Rapid Communications in Mass Spectrometry* 14.15 (2000), pp. 1337–1344.

[17] Dale A Schoeller et al. "Energy expenditure by doubly labeled water: validation in humans and proposed calculation". In: *American Journal of Physiology-Regulatory, Integrative and Comparative Physiology* 250.5 (1986), R823–R830.

[18] Stefano Guidotti et al. “Total energy expenditure assessed by salivary doubly labelled water analysis and its relevance for short-term energy balance in humans”. In: *Rapid Communications in Mass Spectrometry* 30.1 (2016), pp. 143–150.

[19] Christophe Sturm, Qiong Zhang, and David Noone. “An introduction to stable water isotopes in climate models: benefits of forward proxy modelling for paleoclimatology”. In: *Climate of the Past* 6.1 (2010), pp. 115–129.

[20] Sigfus J Johnsen et al. “Greenland palaeotemperatures derived from GRIP bore hole temperature and ice core isotope profiles”. In: *Tellus B: Chemical and Physical Meteorology* 47.5 (1995), pp. 624–629.

[21] Maryvonne L Martin, Gérard J Martin, and Claude Guillou. “A site-specific and multi-element isotopic approach to origin inference of sugars in foods and beverages”. In: *Microchimica Acta* 104.1 (1991), pp. 81–91.

[22] *Commission Regulation (EEC) No 2676/90 of 17 September 1990 determining Community methods for the analysis of wines*. Oct. 1990.

[23] Concetta Pironti et al. “Determination of the 13C/12C carbon isotope ratio in carbonates and bicarbonates by 13C NMR spectroscopy”. In: *Analytical chemistry* 89.21 (2017), pp. 11413–11418.

[24] Henk M De Feyter et al. “NMR visibility of deuterium-labeled liver glycogen in vivo”. In: *Magnetic Resonance in Medicine* 86.1 (2021), pp. 62–68.

[25] GD Cody, CM Alexander, and Susan Wirick. “Approaches to establishing the chemical structure of extraterrestrial organic solids”. In: *Workshop on Cometary Dust in Astrophysics*. 2003.

[26] Gérard J Martin and Maryvonne L Martin. “Climatic significance of isotope ratios”. In: *Phytochemistry Reviews* 2.1 (2003), pp. 179–190.

[27] V Faghihi et al. “A new high-quality set of singly (2H) and doubly (2H and 18O) stable isotope labeled reference waters for biomedical and other isotope-labeled research”. In: *Rapid Communications in Mass Spectrometry* 29.4 (2015), pp. 311–321.

[28] *MestreNova Manual 14.2.3*. URL: `https://mestrelab.com/downloads/mnova/manuals/MestReNova-14.2.3_Manual.pdf`.

[29] Eugenio Alvarado. *Practical Guide for Quantitative 1D NMR integration - U-M LSA*. Oct. 2010. URL: https://lsa.umich.edu/content/dam/chem-assets/chem-docs/Quantitative_NMR.pdf.

[30] Stepan Dzhimak et al. "Determination of Deuterium Concentration in Biological Fluids by NMR Spectroscopy". In: *3rd International Conference on Biological, Chemical Environmental Sciences (BCES-2015)*. 2015, pp. 47–50.

[31] Xiaomin Ma et al. "Direct determination of deuterium of wide concentration range in water by nuclear magnetic resonance". In: *talanta* 97 (2012), pp. 450–455.

[32] GA Kalabin et al. "Determination of deuterium content in components of water-organic solutions by a combination of the NMR 1 and 2 methods". In: *Analytics* 8.2 (2018), pp. 94–100.

[33] Yulia B Monakhova and Bernd WK Diehl. "Novel approach of qNMR workflow by standardization using 2H integral: Application to any intrinsic calibration standard". In: *Talanta* 222 (2021), p. 121504.

[34] Patrick A Hays and Robert A Thompson. "A processing method enabling the use of peak height for accurate and precise proton NMR quantitation". In: *Magnetic resonance in chemistry* 47.10 (2009), pp. 819–824.